

# Zeeman effect of hyperfine-resolved spectral lines of singly ionized praseodymium using collinear laser-ion-beam spectroscopy

S. Werbowy\* and J. Kwela

*Institute of Experimental Physics, University of Gdansk, ulica Wita Stwosza 57, PL-80-952 Gdansk, Poland<sup>†</sup>*

N. Anjum

*Optics Laboratories, P.O. Box 1021, 44000 Nilore, Islamabad, Pakistan<sup>‡</sup>*

H. Hühnermann

*Department of Physics, University of Marburg, Renthof 5, 35037 Marburg, Germany<sup>†</sup>*

L. Windholz<sup>‡</sup>

*Institut für Experimentalphysik, Technische Universität Graz, Petersgasse 16, 8010 Graz, Austria*

(Received 10 June 2014; revised manuscript received 28 August 2014; published 30 September 2014)

Using the high-resolution spectroscopic method of collinear laser-ion-beam spectroscopy (CLIBS), the Zeeman effect of singly ionized praseodymium spectral lines has been studied at relatively small magnetic fields up to 330 G. With this unusual method for studying the Zeeman effect of ionic lines we recorded Zeeman-hyperfine structure patterns with clearly resolved components with linewidths as low as 60 MHz, which is only sometimes the natural linewidth. From the Zeeman patterns of 30 lines, improved Landé  $g_J$  factors were determined for 39 Pr II levels of the  $4f^35d$ ,  $4f^25d^2$ , and  $4f^36p$  configurations.

DOI: [10.1103/PhysRevA.90.032515](https://doi.org/10.1103/PhysRevA.90.032515)

PACS number(s): 32.10.Fn, 32.60.+i

## I. INTRODUCTION

Praseodymium is a rare-earth element with only one stable isotope having atomic mass number 141 and 59 electrons. Because of its electronic properties, the number of all classified as well those still unclassified transitions in the UV-IR spectral region is an average 400 lines per 1000  $\text{cm}^{-1}$  [1]. Moreover, there are certain regions (i.e., around 400 and 1000 nm) with exceptionally dense spectra, with more than 1000 lines per 1000  $\text{cm}^{-1}$  [1]. Besides atomic lines, many lines of the first ion are contained in emission spectra, in the range 2783–27920  $\text{cm}^{-1}$  the number of intense classified lines of Pr II is 878 [1]. The theoretical predictions give rise to 854 possible even and odd levels for energies up to 35497  $\text{cm}^{-1}$  [2]. For many years, there have been ongoing investigations to observe and classify all levels of praseodymium [3–5] as well of its first ion [6–9]. This task is very difficult and time consuming, and from time to time some investigators report the discovery of new levels or lines.

Due to the large density of observed transitions and the complex hyperfine (hf) structure, at the beginning, the high-current arc source emission spectra were resolved using classical spectroscopic techniques like large spectrographs (i.e., diffraction grating in fourth order of a 75-ft spectrograph [10]). Patterns were recorded on photographic plates. This allowed accurate analysis only for the strongest transitions. Later, high-resolution Fourier-transform spectrometers were used [1].

With the development of narrow-band tunable lasers, the accuracy of hyperfine structure investigations has been

significantly improved. Narrow-band laser light enables us to excite certain upper levels and to study their decay, instead of classical broad-band excitation in a discharge. The selective excitation allows us to drive only one transition (or several transitions having by chance nearly the same wave number) and to identify the populated levels by their fluorescence decays. Two main techniques are used: (i) Doppler-free spectroscopy on atomic or ionic beams or in trapping devices and (ii) Doppler-limited spectroscopy, using as a source of free atoms a hollow cathode discharge lamp, which is a working horse because it gives access to a larger number of levels.

The theoretical interpretation of the level structures of Pr I and Pr II is difficult. Levels of different configurations overlap each other. This causes significant disagreement between experimentally found and theoretically calculated level energies [2]. The differences are tens and sometimes hundreds of  $\text{cm}^{-1}$ , which makes the classification of experimental levels difficult. Thus the classification should be supported by comparing not only energies but also other spectroscopic parameters. For the classification of a spectral line as a transition between two combining levels, the observed hyperfine pattern of the line is very useful. It allows us to distinguish the involved levels in blend situations and it gives access to their quantum numbers  $J$  [11]. The isotope shifts are also useful parameters for elements having several isotopes. Unfortunately, this is not the case for praseodymium. Calculations of the hyperfine structure constants or isotope shifts of a level (either *ab initio* or by a semiempirical least-squares fitting procedure for adjusting the Slater parameters) require special attention and theoretical treatment, because they involve parameters representing the radial part of the wave functions.

Fortunately, with the help of theoretical calculations the Landé factors can also be determined. To calculate them, no radial part of the wave function is required. For this reason

\*dokws@univ.gda.pl

<sup>†</sup>Also at Institut für Experimentalphysik, Technische Universität Graz, Petersgasse 16, 8010 Graz, Austria.

<sup>‡</sup>windholz@tugraz.at

the Landé factors  $g_J$  are very helpful for level classification. Additionally,  $g_J$  indicates any deviation from pure  $LS$  coupling and allows us to make quantitative estimations on the composition of eigenfunctions in intermediate coupling.

Although there are a large number of investigations concerning hyperfine structure, new levels, and  $J$  quantum number determination [3–5,9] (and references therein), there seems to be a big gap in determining or improving Landé factors  $g_J$ , which are essential for proper and complete classification of the level.

All of the literature data on the Zeeman effect of Pr II comes from Doppler-limited spectroscopy and from arc discharge sources [1,12]. Rosen *et al.* [12] investigated the Zeeman effect of Pr II lines in magnetic fields up to 95000 G and determined  $g_J$  factors for 74 levels from resolved Zeeman patterns of 141 lines in the range 2400 to 7100 Å. For lines showing a complex hyperfine structure high magnetic fields are necessary to make the Zeeman splitting much higher than the hf splitting. Ginibre [1] has reinvestigated the experimental material stored on photographic plates recorded earlier in fields of 23 000 G and determined  $g_J$  values for 236 levels of Pr II. In her analysis of Zeeman patterns she had to analyze the patterns of several lines simultaneously, due to the hf structure and the high density of the spectral lines. She could measure only distances between specific polarized components. Using simplified relationships concerning the Zeeman effect unperturbed by hf structure splitting, she has obtained values of  $g$  factors which, in her opinion, are not accurate enough and should be treated only as guides for the classification of the lines [1].

In this paper we have investigated the Zeeman effect at magnetic fields up to 330 G, which are very small compared to the fields used in Refs. [1,12]. Thus we have not investigated the hf structure of the Zeeman effect of the fine structure levels but the Zeeman effect of the hf structure levels. Consequently we had to use an experimental method with a high spectral resolution (Doppler-effect reduced spectroscopy) and a complex analysis of the observed Zeeman-hf patterns to obtain Landé  $g$  factors. We performed our investigations by a method rather unusual for Zeeman-effect investigations, namely, collinear laser ion-beam spectroscopy combined with Doppler tuning.

In general, this technique allows for high-resolution investigations of hf structures as well as isotope shifts for ions. But we could find only one paper [13] which reports use of this method for Zeeman-effect investigations. One reason may be the general belief that applying a magnetic field perpendicular to the ion beam causes a beam deflection which may lead to an unacceptable broadening of the spectral lines. Such deviation is avoided by applying a magnetic field oriented parallel to the ion path, as it was done for Ba<sup>+</sup> ions [13]. Consequently, only  $\Delta M = \pm 1$  components, excitable with circularly polarized light ( $\sigma_{\pm}$ ), can be observed in this way.

However, if we consider a large ion mass (as having Pr ions, 141 atomic units), kinetic energies around 20 keV and the fact that the perpendicular magnetic field interacts with the ions only in the small part of the ion-beam path where the ions are excited by laser light and fluorescence is observed (length about 50 mm), we find that after 50 mm the deviation from the

original path is smaller than 0.1 mm, even for fields as high as 500 G. Thus it is possible to apply magnetic fields of this order of magnitude perpendicular to the ion beam and to perform a standard Zeeman-effect analysis of the selected transition by observing both polarized components ( $\Delta M = 0, \pm 1, \pi$ , and  $\sigma$ ) with high resolution.

The possibilities of collinear laser-ion-beam spectroscopy (CLIBS) for Zeeman-effect investigations were demonstrated in this paper on Pr ions. Pr was selected for several reasons: (i) the group in Graz has experience related to this ion [6–9,14], (ii) very accurate  $g_J$  factors are not available for most of the Pr II levels, and (iii) the determined factors may contribute to a better designation of the involved levels.

## II. EXPERIMENT

The measurements were performed on the CLIBS apparatus which was named the Marburg separator MARS-II, originally installed at the University of Marburg a.d. Lahn (Germany) and moved in the year 2002 to Graz (Austria). For many years it has been used for investigations of hf structures and isotope shifts of lines of different singly ionized heavy elements. Details of the apparatus were described recently in [14]. Figure 1 presents the scheme of the experimental setup. Briefly, it is composed of a surface ionization ion source, where the element to be investigated is contained in powder form and is heated to produce metal vapor. The vapor then passes through a thin hot tube and some of the atoms become ionized. The ions are extracted and accelerated by a voltage of ca. 20 kV, and a beam is formed by means of some ion optics lenses. Then the ion beam passes a huge magnet which separates the paths of different isotopes, and the ions of the desired isotope travel into the interaction chamber, which is located 6.5 m from the ion source. At such conditions, the ions arrive after app. 38  $\mu$ s after being ionized in the source. This means that the ions arriving at the interaction chamber are only in the ground or in metastable states. The typical ion current densities were of the order of 0.1 nA/mm<sup>2</sup>, but for some transitions we needed currents as high as 6 nA/mm<sup>2</sup> to obtain a good signal to noise ratio.

In the interaction chamber the ions are overlapped with a counterpropagating laser light beam, produced by a narrow band ring-dye laser (Rhodamine 6 G dye was used for the given wavelength range, laser linewidth about 1 MHz, typical power density 15 mW/mm<sup>2</sup>), stabilized, and fixed to a certain wave number (app. 9 cm<sup>-1</sup> Doppler shift must be taken into account due to the high ion velocity). The ions were excited from metastable odd levels of the  $4f^35d$  configuration to even levels of the  $4f^36p$  configuration, and their fluorescence decay was observed (see Fig. 2). With a set of a Glan-Taylor prism and a half-wave plate we produced laser light polarized in a direction perpendicular ( $\sigma$  component) and parallel ( $\pi$  component) to the magnetic field direction. For suppressing laser stray light and background light generated by collisions of the ions with the rest of the gas atoms a Schott BG-12 glass filter was used in front of the photomultiplier detecting laser-induced fluorescence.

The hyperfine pattern of the investigated transitions were recorded using the Doppler tuning technique. By post-accelerating the ions in the interaction region it is possible

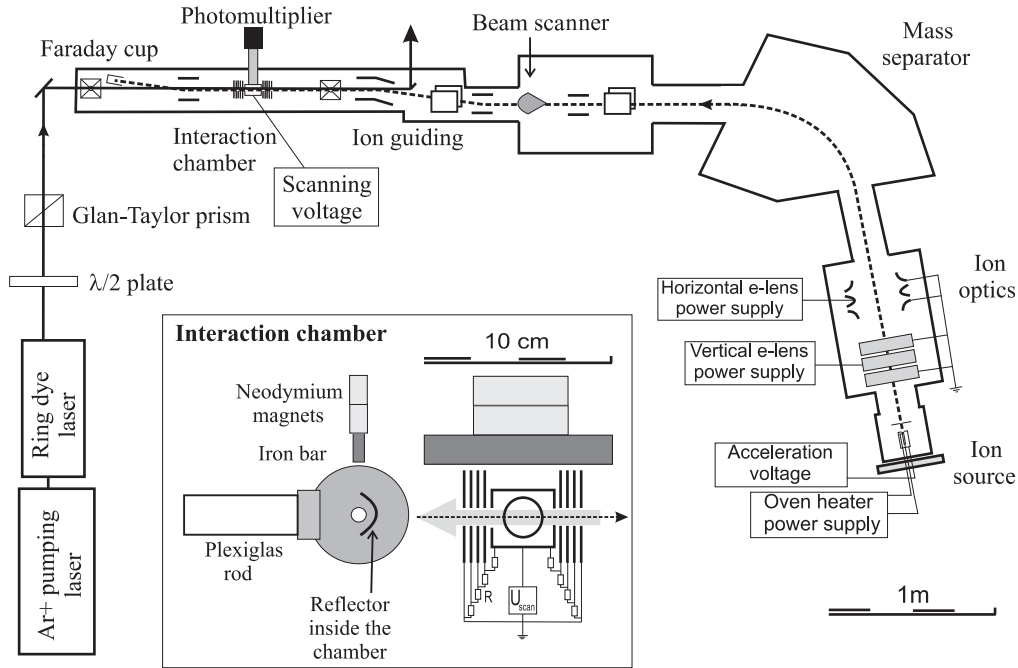


FIG. 1. Experimental setup of MARS-II apparatus.

to change the Doppler shift of the laser frequency noticed by the ions. Increasing the original kinetic energy step by step by altogether 3.5 keV, we could perform a scan of the wave number of app.  $0.75 \text{ cm}^{-1}$  (22 GHz) with a step size as small as 5 MHz. The frequency position of the components can be directly obtained from the acceleration voltage  $U_{\text{acc}}$  and the applied postacceleration scanning voltage  $U_{\text{scan}}$  according to the formula

$$\begin{aligned} \Delta\nu_{\text{DS}}(U_{\text{scan}}) &= \nu_L(U_{\text{scan}}) - \nu_0 \\ &= \frac{\nu_0}{c} \sqrt{\frac{2}{M}} (\sqrt{U_{\text{acc}} + U_{\text{scan}}} - \sqrt{U_{\text{acc}} + U_{\text{scan}}^0}), \end{aligned} \quad (1)$$

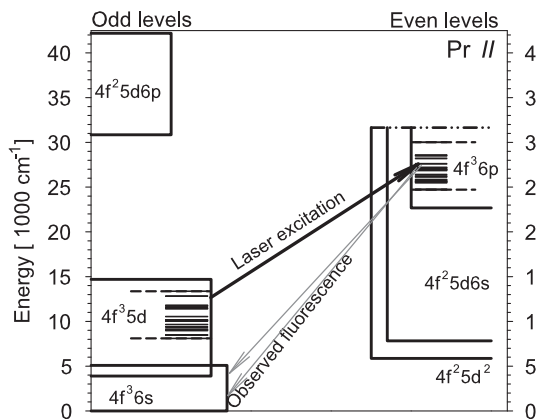


FIG. 2. Even and odd configurations of Pr II [1]. Dashed lines indicate the range of the investigated metastable levels of the  $4f^3 5d$  configuration and that of  $4f^3 6p$ . Arrows present the laser excitation from the metastable levels of  $4f^3 5d$  to  $4f^3 6p$  levels, from which the fluorescence to ground  $4f^3 6s$  configuration is collected.

where  $\nu_0$  is the transition wave number,  $M$  is the mass of the ion, and  $U_{\text{scan}}^0$  is the scanning voltage of the first point.

The magnetic field in the interaction region was produced by a set of permanent neodymium magnets together with a ferromagnetic bar as the magnetic pole, placed outside the interaction chamber (see Fig. 1). In this way we avoided difficulties with vacuum contamination and made the system

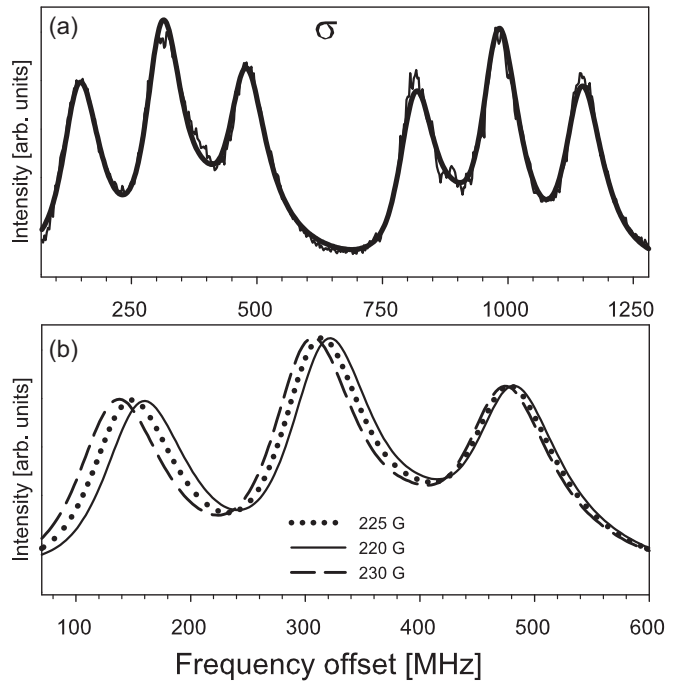


FIG. 3. (a) Recorded Zeeman pattern and the computer best fit at 225 G of the  $^{138}\text{Ba II}$  5853.68 Å transition used for the magnetic field check. (b) Calculated Zeeman patterns for the line for 220, 225, and 230 G fields (only first three components from the left are shown).

very simple. By simply changing the arrangement of magnets we could produce uniform fields of different strengths. The strength and distribution of the magnetic field was measured with a Hall-effect Gauss-meter Applied Magnetics Laboratory model GM1A (probe model PB71-10) with accuracy of 0.25% of reading. Along the region in which the ions are Doppler tuned into resonance with the exciting laser light (length 30 mm) the field does not change by more than 1 G.

Additionally, the magnetic field strength was checked by measurements on the Ba II transition  $5853.68 \text{ \AA}$  ( $6p^2P_{3/2} \rightarrow 5d^2D_{3/2}$ ). The recorded Zeeman hf pattern is shown in Fig. 3(a), together with the results of a least-squares fit. The Landé factor for the upper level is  $0.7993278(3)$  [15]. For the lower level there are two independently measured consistent values available:  $1.328(8)$  from time-differential level-crossing measurements [16] and  $1.325(11)$  [13], from “in-flight” saturated absorption laser spectroscopy. Simulations of the Ba II line presented in Fig. 3(b) shows how sensitive the structure of this line is concerning variations of the magnetic field. A

change of the field strength by 5 G shifts the position of the outer components by app. 10 MHz.

From simulations of this Ba II line we found that a change of the  $g_J$  factor of the lower  $^2D_{3/2}$  level,  $1.328(8)$ , by  $\pm 0.008$  units affects the determined magnetic field by  $\pm 0.5\%$ . Combining the uncertainties from the measurements performed with our Gauss-meter ( $\pm 0.25\%$ ) and from evaluation of the Ba II line ( $\pm 0.5\%$ ), using the RRS method (square root of the sum of the squares) [17] we estimate the accuracy of the field determination to be  $\Delta B/B = \pm 0.56\%$ . On this basis, the strengths of the used fields are  $225(1.3)$  and  $330(2)$  G.

### III. RESULTS AND DISCUSSION

Zeeman hf structure patterns for 30 lines of  $^{141}\text{Pr II}$  in the region  $5815.17\text{--}6017.81 \text{ \AA}$  were recorded. The transitions were excited both with  $\sigma$  ( $\Delta M = \pm 1$ ) and  $\pi$  ( $\Delta M = 0$ ) polarized light. Examples of such records together with calculated best fits for two Pr II transitions ( $5815.17$  and  $5951.77 \text{ \AA}$ ) are presented in Figs. 4 and 5 (please note the enormous number of Zeeman hf structure components). As can be seen from the figures, the small magnetic fields used in this work are high enough to produce significant changes in the patterns, allowing an accurate determination of the Landé factors. While for zero field the hf patterns have only few components, the magnetic field separates the different  $\Delta M$  components,

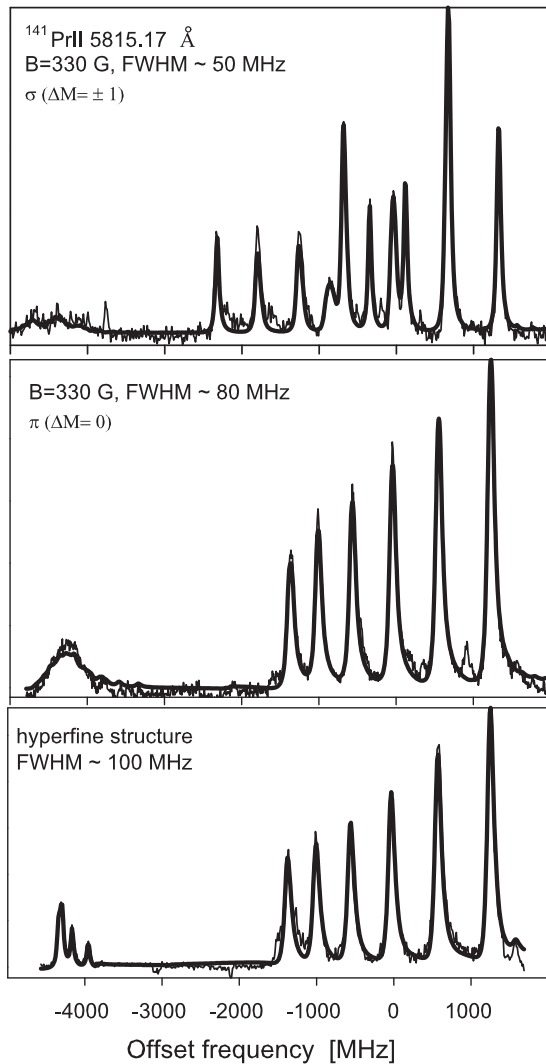


FIG. 4. Recorded Zeeman-hf structure pattern of the Pr II line  $5815.17 \text{ \AA}$  at 330 G. The thin line represents the experimental result and the thick line the computer best fit. In the lowest trace the hf pattern of this line is shown (field free).

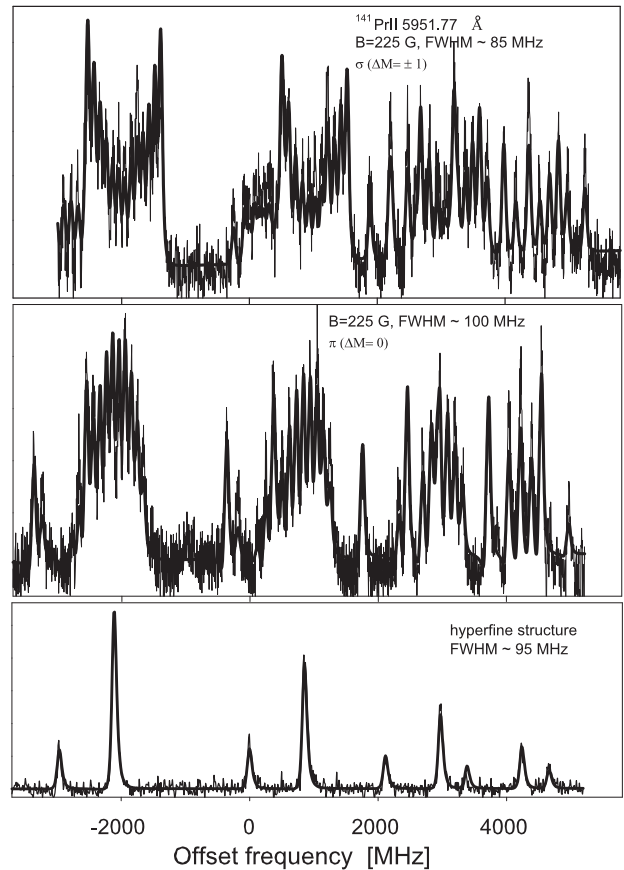


FIG. 5. Recorded Zeeman-hf structure pattern of the Pr II line  $5951.77 \text{ \AA}$  at 225 G. The thin line represents the experimental result and the thick line the computer best fit. In the lowest trace the hf pattern of this line is shown.

TABLE I. Landé  $g_J$  factors of singly ionized praseodymium for even energy levels ( $\geq 24716.093 \text{ cm}^{-1}$ ) having the leading configuration  $4f^3(^4I^o)6p$  and for odd energy levels ( $\leq 13373.652 \text{ cm}^{-1}$ ) having the leading configuration  $4f^3(^4I^o)5d$ . A question mark indicates that the configuration or term assignment is not known or questionable.

Level energy <sup>a</sup> ( $\text{cm}^{-1}$ )	Term <sup>b</sup>	Excitation wavelengths ( $\text{\AA}$ )	Experimental $g_J$			Theoretical $g_J$	
			Present studies	Ref. [1] <sup>c</sup>	Ref. [12] <sup>d</sup>	Ref. [2] HFR	$LS$ coupling
30018.138	$^5H_7?$	6006.33, 5815.33	1.211 (16)	1.215	1.215	1.193	1.286
28577.821	$^3I_7?$	5940.73, 5892.24	1.180 (18)	1.19	1.187		1.143
28508.823	$^3I_6$	5981.19, 5859.68	1.085 (10)	1.09	1.103	1.087	1.024
28201.980	$^5I_8$	5956.61	1.158 (13)	1.165	1.154		1.25
27604.990	? $J = 6$	5856.908	1.066 (12)	1.13			
27198.297	? $J = 5$	5852.63	1.042 (10)	1.07	1.067	1.047	
27128.016	$^5K_8$	5847.13	1.142 (10)	1.15	1.143	1.152	1.153
26973.549	$^5H_5$	5930.66, 5947.19	1.085 (11)	1.12	1.101	1.075	1.10
26962.021	$^3H_6$	5951.27	1.055 (11)	1.08	1.073	1.001	1.167
26860.974	$^5I_7$	5939.90	1.122 (7)	1.115	1.123	1.124	1.179
26398.569	? $J = 6$	5967.82, 5873.83	0.961 (7)	0.99	0.99		
26226.628	? $J = 4$	5847.05, 5818.57	0.887 (10)	0.91		0.909	
25842.444	? $J = 5$	5981.46	1.026 (8)	1.00	0.999	1.041	
25762.825	? $J = 3$	5980.00, 5951.77	0.842 (5)	0.86			
25656.737	$^5I_6?$	5815.17, 5823.58	1.033 (7)	1.05	1.042		1.071
25610.227	$^5H_6$	5830.95	1.126 (11)	1.12	1.116	0.98	1.214
25578.507	$^5H_3$	6017.81	0.530 (9)	0.55			0.50
25499.570	? $J = 5$	5877.39, 5868.82	0.960 (8)	0.995	0.984		
24755.017	? $J = 4$	6002.43	0.910 (7)	0.905	0.911	0.922	
24716.093	$^5I_5$	6016.49	0.896 (9)	0.915	0.911		0.90
13373.648	$^3K_8$	6006.33	1.160 (17)	1.14	1.231		1.125
12826.982	$^5G_6$	5815.33	1.320 (50)	1.285			1.333
11794.384	$^3K_7$	5981.19	1.060 (16)	1.12			1.018
11749.526	$^3L_6$	5940.73	1.240 (29)	1.215			0.667
11611.054	$^5I_8$	5892.24	1.125 (11)	1.236			1.25
11447.788	$^5G_5$	5859.68	1.184 (13)	1.20			1.267
11418.672	$^3L_7$	5956.61	1.110 (18)	0.897			0.875
10535.868	? $J = 5$	5856.908	1.041 (14)	1.11			
10163.531	$^3K_6$	5947.19, 5951.27	0.920 (8)	0.93			0.857
10116.696	$^5G_4$	5930.66, 5852.63	1.031 (10)	1.07			1.15
10030.351	? $J = 7$	5939.90, 5847.13	1.150 (8)	1.14			
9646.679	$^5I_6$	5967.82	1.046 (8)	1.076	1.073		1.071
9378.612	$^5H_5$	5873.83	1.036 (7)	1.05	1.044		1.10
9128.741	? $J = 4$	5981.46, 5874.74, 5847.05	0.906 (6)	0.91			
9045.051	$^5G_3$	5818.57, 5980	0.821 (11)	0.83			0.917
8965.764	$^5G_2$	6017.81, 5951.77	0.343 (2)	0.37			0.333
8489.934	$^5I_5$	5823.58, 5877.39	0.890 (31)	0.93	0.93		0.90
8465.102	$^3I_6$	5830.95, 5815.17, 5868.82	1.025 (7)	1.035			1.024
8099.697	$^5H_4$	6002.43, 6016.49	0.820 (8)	0.83			0.90

<sup>a</sup>Energy values are taken from Ref. [9], experimental uncertainties are  $0.005 \text{ cm}^{-1}$ .

<sup>b</sup>Terms assignment after NIST Standard Reference Data [22].

<sup>c</sup>Experimental uncertainties were not given in Ref. [1].

<sup>d</sup>Observed in Ref. [12]  $g_J$  values are in most cases believed to be correct to within an average deviation of  $\pm 0.005$  unit.

which number runs into the hundreds. Such a large number of observed Zeeman hf structure transitions makes it impossible to analyze its structure without appropriate computer software. To analyze the data we have used a software developed in our group (by S. Werbowy) which was used extensively earlier in the analysis of the Zeeman hf structure of other elements [18–20]. In the least-squares-fitting procedure we used very accurate hyperfine structure constants  $A$  and  $B$  determined on the same experimental setup and published in [14]. We also

used a special asymmetric line profile

$$I(\nu) = I_{bc} + \sum_i \frac{I_{0,i} [1 + \chi/\alpha_1 (\nu - \nu_0^i - \tilde{\nu})]}{1 + [\alpha_1 (\nu - \nu_0^i - \tilde{\nu})]^2 + [\alpha_2 (\nu - \nu_0^i - \tilde{\nu})]^4}, \quad (2)$$

where  $I_{0,i}$  and  $\nu_0^i$  are the intensity and position of a single component calculated from the diagonalization of a Zeeman hf structure Hamiltonian matrix (for details see [18]),  $\alpha_i = 2/\delta\nu_i$  is a line-shape parameter,  $\delta\nu_1$  is directly

the full linewidth at half maximum,  $\tilde{\nu}$  shifts the entire hf pattern. The experimental FWHM linewidth  $\delta\nu_1$  varied in the range 50–100 MHz. The parameter  $\chi$  describes the asymmetry of the line due to nonsymmetric velocity speed distribution of the ion beam, and its typical value was 0.00015.

A summary of the obtained Landé  $g_J$  factors is presented in Table I. The table contains the energy of the level, its designation (if known), quantum number  $J$ , excitation wavelengths involving the given level, and experimental values of  $g_J$  factors obtained in this work. For comparison, values known from the literature are given. The table contains also numbers from pseudorelativistic Hartree-Fock calculations (HFR) and determined for pure  $LS$  coupling.

The presented experimental results are the mean values from several independent measurements of  $\sigma$  and  $\pi$  components, made sometimes at different days at different transitions. The given experimental uncertainties combine the contributions from mean standard deviations and the uncertainties of field determination  $g_J(\Delta B/B)$ . Here also the RRS method [17] was used. Present experimental uncertainties are different for each level, in the range from 0.002 to 0.05. This wide span of uncertainty results from various factors, such as the signal-to-noise ratio of the recorded structure, and if the investigated line has an hf pattern influenced in a distinct way by the magnetic field. Since each line's hf pattern mirrors the Zeeman patterns of both combining levels, sometimes the effects of upper and lower levels nearly cancel each other. Nevertheless, for all observed lines the  $\sigma(\Delta M = \pm 1)$  patterns show high sensitivity on variation of  $g_J$  of the involved levels. In contrast to  $\sigma$ , the  $\pi(\Delta M = 0)$  patterns not always show this sensitivity. For those cases, the pattern of the Zeeman hf  $\pi$  components are not very different to the hf patterns without external magnetic field (that is the case if Landé  $g_J$  factors of upper and lower levels are close to each other, see Fig. 4). In such cases, the uncertainty of our results was much higher, and we mainly focused on investigations of the  $\sigma(\Delta M = \pm 1)$  components.

Considering the difficulties which the authors of Ref. [12] had to overcome (i.e., the very dense Pr II emission spectrum, the presence of Pr I lines, the inaccuracy of hyperfine structure constants, the lack of computer analysis resulting in a poor interpretation of the patterns recorded using standard photographic technique, and scaling the magnetic field on measurements of the strongest transitions of silver, copper, and calcium) in our opinion their uncertainties are underestimated. Although the present experimental uncertainties are in most cases higher than given in Ref. [12], we believe that our results are more reliable.

For the Pr II spectrum neither  $LS$  nor  $jj$  coupling is adequate. The  $g_J$  factors calculated in  $LS$  coupling are given in column 8 of Table I. A comparison between calculated and experimental  $g_J$  values gives information about the degree of departure from  $LS$  coupling. Deviations between these two values in Pr II are not very significant for most cases. This is in contrast to Nd II, where breakdown of  $LS$  coupling is observed; many eigenfunctions in the intermediate coupling have leading components smaller than 10% [21].

The sum of  $g_J$  factors for all levels of a given configuration having one and the same value  $J$  does not depend on the

TABLE II. Suggestions of term assignment for levels from Table I, in the  $LS$  coupling scheme.

Level energy (cm <sup>-1</sup> )	$g_J$ -Present studies	Possible term label	$g_J - LS$ coupling
27604.989	1.066 (11)	<sup>5</sup> I <sub>6</sub>	1.071
27198.298	1.042 (9)	<sup>3</sup> H <sub>5</sub>	1.033
26398.568	0.961 (5)	<sup>5</sup> K <sub>6</sub>	0.905
26226.627	0.887 (9)	<sup>5</sup> H <sub>4</sub>	0.900
25842.444	1.026 (6)	<sup>3</sup> H <sub>5</sub>	1.033
24755.017	0.910 (6)	<sup>5</sup> H <sub>4</sub>	0.900
10535.866	1.041 (13)	<sup>3</sup> H <sub>5</sub>	1.033
10030.350	1.150 (5)	<sup>3</sup> I <sub>7</sub>	1.143
9128.742	0.906 (4)	<sup>5</sup> H <sub>4</sub>	0.900

type of coupling. Because deviations between  $g_J$  values calculated in  $LS$  coupling and experimental  $g_J$  values are not very significant, also sums for a given  $J$  of calculated and experimental  $g_J$  differ not too much. It implies that a  $g_J$  transfer to other configurations is weak.

As can be seen in Table I, the term assignment in the NIST data bank [22] is sometimes not given. Using the fact that the deviations from the  $LS$  coupling scheme are not significant we have attempted to determine missing designations of several levels of Pr II. For this purpose, for different combinations of values for quantum numbers  $L$ ,  $S$ , and  $J$ , the  $g_J$  factors have been calculated. Next, by comparison with experimental values the best fitting calculated results have been selected. Results of this analysis are presented in Table II.

#### IV. CONCLUSIONS

Using collinear ion-beam spectroscopy we have investigated the Zeeman effect of 30 lines of Pr II in magnetic fields of 225(1.3) and 330(2) G, oriented perpendicular to the ion beam. From the detailed analysis of the recorded high-resolution Zeeman hf structure patterns we have determined the Landé  $g_J$  factors for 39 levels of Pr II.

We also demonstrated successful that a CLIBS apparatus can be used to investigate the Zeeman effect of an hf pattern of a spectral line, applying relatively small perpendicular magnetic field (up to a few hundred Gauss) in a small laser interaction region (few mm) of an ion beam. Such a field does not produce a significant beam deviation leading to unacceptable broadenings of the line components and to a misalignment of the counterpropagating laser and ion beams. We hope that this work will encourage other researchers to perform Zeeman-effect investigations using collinear ion-beam spectroscopy.

#### ACKNOWLEDGMENTS

The present work was supported by Wissenschaftlich-Technische Zusammenarbeit Österreich-Polen, Projects No. PI 21/2012 and No. PI 12/2014. N.A. acknowledges the support of the Higher Education Committee, Pakistan, for enabling PhD studies at the University of Technology, Graz.

- [1] A. Ginibre, *Phys. Scr.* **39**, 694 (1989).
- [2] E. Biémont *et al.*, *Eur. Phys. J. D* **27**, 3341 (2003).
- [3] K. Shamim, I. Siddiqui, and L. Windholz, *Eur. Phys. J. D* **64**, 209 (2011).
- [4] T. I. Syed *et al.*, *Phys. Scr.* **84**, 065303 (2011).
- [5] I. Siddiqui, K. Shamim, and L. Windholz, *Eur. Phys. J. D* **68**, 122 (2014).
- [6] B. Gamper *et al.*, *J. Phys. B* **44**, 045003 (2011).
- [7] B. Furmann *et al.*, *Phys. Scr.* **72**, 300 (2005).
- [8] B. Furmann, D. Stefanska, J. Dembczynski, and E. Stachowska, *At. Data Nucl. Data Tables* **93**, 127 (2007).
- [9] N. Akhtar and L. Windholz, *J. Phys. B* **45**, 095001 (2012).
- [10] H. E. White, *Phys. Rev.* **34**, 1397 (1929).
- [11] L. Windholz, *J. Phys. B: At., Mol. Opt. Phys.*, <http://iopscience.iop.org/0953-4075/labtalk-article/49542> (IOP Publishing).
- [12] N. Rosen, G. R. Harrison, and J. R. McNally, Jr., *Phys. Rev.* **60**, 722 (1941).
- [13] M. Larzilliere, M. Carre, and M. L. Gaillard, *Opt. Commun.* **37**, 27 (1981).
- [14] N. Akhtar, N. Anjum, H. Hühnermann, and L. Windholz, *Eur. Phys. J. D* **66**, 264 (2012).
- [15] K. H. Knöll, G. Marx, K. Hübner, F. Schweikert, S. Stahl, C. Weber, and G. Werth, *Phys. Rev. A* **54**, 1199 (1996).
- [16] O. Poulsen and P. S. Ramanujam, *Phys. Rev. A* **14**, 1463 (1976).
- [17] B. N. Taylor and C. E. Kuyatt, *Guidelines for Evaluating and Expressing the Uncertainty of NIST Measurement Results* (U.S. Government Printing Office, Washington, DC, 1994).
- [18] S. Werbowy *et al.*, *Eur. Phys. J. D* **39**, 5 (2006).
- [19] S. Werbowy and J. Kwela, *Phys. Rev. A* **77**, 023410 (2008).
- [20] S. Werbowy and J. Kwela, *J. Phys. B* **43**, 065002 (2010).
- [21] J. Blaise and J. F. Wyart, *Phys. Scr.* **29**, 119 (1984).
- [22] W. C. Martin, R. Zalubas, and L. Hagan, *Atomic Energy Levels—The Rare-Earth Elements*, NSRDS-NBS 60 (US GPO, Washington, 1978).